Materials Research Proceedings 41 (2024) 1144-1149 https://doi.org/10.21741/9781644903131-126

Measurement of shear deformation behavior in thickness direction for a mild steel sheet

HAKOYAMA Tomoyuki[1,a *], HAKOYAMA Chiharu[2,b] and FURUSATO Daichi[3,c]

[1]Tokai National Higher Education and Research System, Gifu University, 1-1 Yanagido, Gifu, 501-1193, Japan

[2]Chubu University, 1200 Matsumoto-cho, Kasugai-shi, Aichi, 487-8501, Japan

[3]Graduate student, Tokai National Higher Education and Research System, Gifu University, 1-1 Yanagido, Gifu, 501-1193, Japan

[a]hakoyama.tomoyuki.s7@f.gifu-u.ac.jp, [b]c_hakoyama@isc.chubu.ac.jp, [c]furusato.daichi.u8@s.gifu-u.ac.jp

Keywords: Material Modeling, Plate Forging, Shear Deformation

Abstract. The anisotropy parameter of the through-thickness shear for a hot-rolled mild steel sheet was determined by comparing the measured and simulated deformation behaviors. A tensile test using a strip specimen with a stepped shape in the thickness direction to apply the through-thickness shear deformation at the center of the specimen was conducted. Finite element analyses were performed by changing the anisotropy parameter *M* of the Hill '48 yield function. The measured through-thickness shear strain γ_{zx} was compared with the simulated one to identify the parameter *M*. In addition, plate compression simulations were performed to evaluate the effect of the through-thickness shear anisotropy on the deformation behavior during plate compression.

Introduction

Plate forging (sheet-bulk metal forming), which is a hybrid process of sheet metal forming and forging, is used to manufacture parts with complex shapes. In plate forging, the same accuracy as that of machining is required [1]. The use of finite element analysis is crucial for realizing trial-and-error-less manufacturing in plate forging.

One of the authors [2] investigated the deformation behavior during a plate compression test with a large-diameter circular plate relative to its thickness. The measured thickness distribution and change in diameter during plate compression are in qualitative agreement with the simulated values. On the other hand, there are some quantitative discrepancies between the experiment and simulation results. Improving the representation accuracy of material models is vital for enhancing the precision of plasticity simulations [3].

A crucial deformation mode in the forging process is shear deformation. Since the surface of the workpiece is constrained by friction between the workpiece and the tool, large through-thickness shear deformation occurs during plate forging. Fig. 1 shows the simulated through-thickness shear strain distribution during plate compression. The simulation conditions for Fig. 1 are the same as those in the reference [2]. The constraint by friction results in a maximum shear strain of approximately 0.15 in the through-thickness direction on the material surface near the plate edge when the plate is compressed by approximately 10%.

Lattanzi et al. [4] measured the strain distribution during the shearing process using digital image correlation (DIC) and identified a through-thickness shear anisotropy parameter of the Hill '48 yield function [5] based on finite element model updating (FEMU). In the identification using shearing processing, since the effect of the constraint at the material edge on the strain distribution is significant, a long test specimen is required. Then the shear strain attained is relatively small.

In this study a through-thickness shear anisotropy parameter of the Hill '48 yield function was identified using a testing method with the tensile test type specimen. A tensile test using a strip specimen with a stepped shape in the thickness direction to apply the through-thickness shear deformation at the center of the specimen was conducted. Finite element analyses (FEAs) of the tensile test were performed by changing the anisotropy parameter *M* of the Hill '48 yield function. The variation of the measured through-thickness shear strain γ_{zx} during tensile test was compared with the simulated one to identify the parameter *M*. In addition, plate compression simulations using the best parameter of *M* were performed to evaluate the influence of the through-thickness shear anisotropy on the deformation behavior of plate compression.

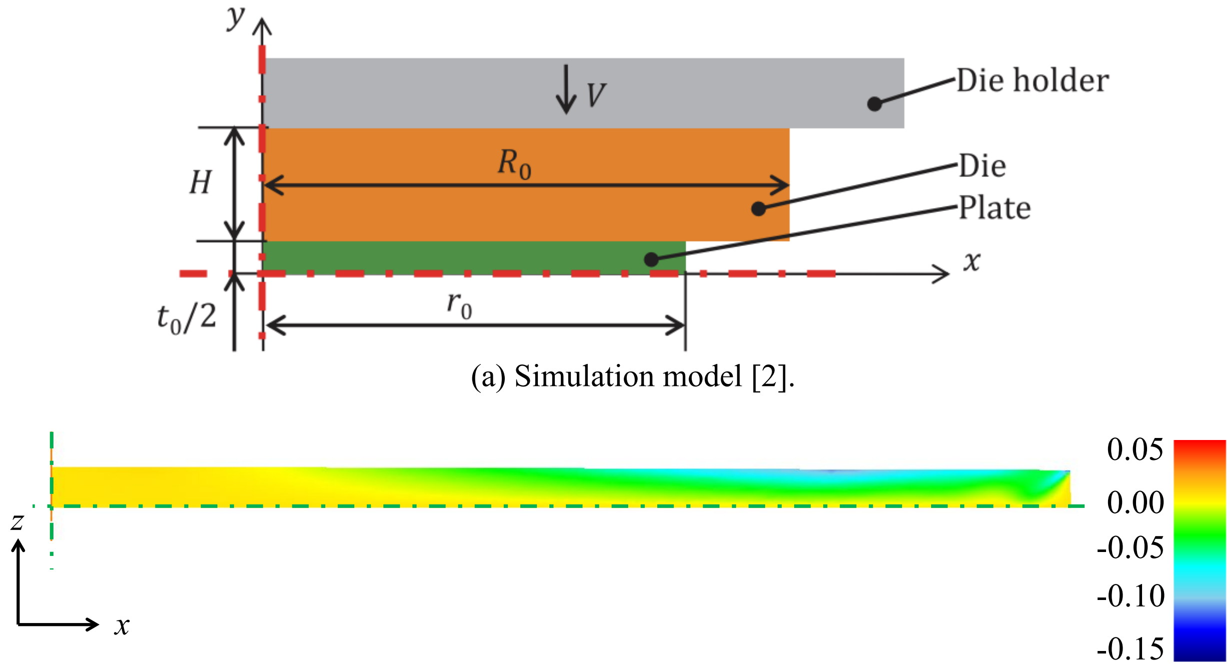

(a) Simulation model [2].

(b) Shear strain γ_{zx} distribution in the plate.

Figure 1 Through-thickness shear strain distribution during the plate compression test.

Experimental conditions

Test material. The material used in this study was a commercial hot-rolled mild steel sheet SPHC (nominal thickness t_0 = 2.3 mm). In order to investigate the work hardening behavior of this material, a uniaxial tensile test was conducted. The testing apparatus used was the Autograph AG-50kN X plus (Shimadzu corporation). A strain gage was attached to the center of the test specimen to measure the longitudinal strain. The stress–strain curve measured by the tensile test is shown in Fig. 2. Swift's work hardening law was approximated from the testing result (eq. (1)).

Hereafter, the rolling direction is referred to as *x*, the transverse direction as *y*, and the thickness direction as *z*.

$$\sigma = \begin{cases} 383\ \mathrm{MPa} & \text{for } \varepsilon_0^{\mathrm{p}} < 0.025 \\ 721\left(\varepsilon_0^{\mathrm{p}} + 0.0007\right)^{0.17}\ \mathrm{MPa} & \text{for } \varepsilon_0^{\mathrm{p}} \geq 0.025 \end{cases}, \quad (1)$$

where $\varepsilon_0^{\mathrm{p}}$ is the reference plastic strain.

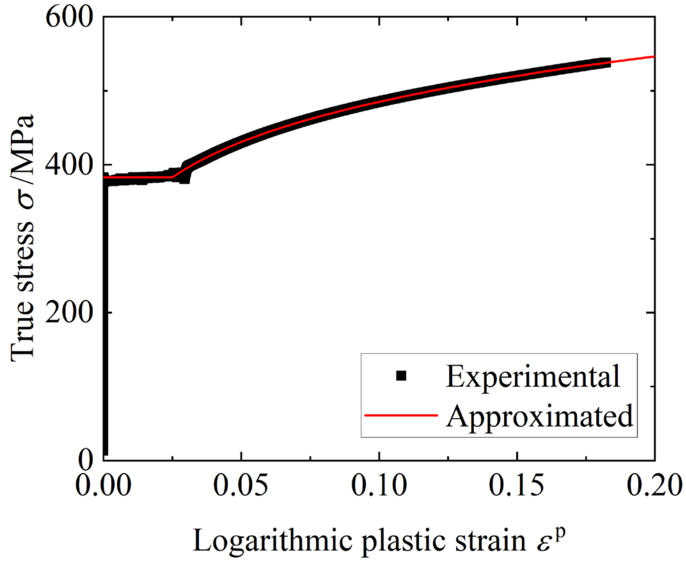

Figure 2 True stress-logarithmic plastic strain curves measured and approximated.

Specimen for the measurement of shear deformation behavior. The shape of the specimen used in this study is shown in Fig. 3. By applying tensile force to both ends of the specimen, shear deformation can be probed in the centoral zone of the specimen. Based on the FEA results, the dimensions of the specimen were optimized to achieve the largest possible shear strain within the manufacturing constraints (L = 50 mm, l = 1.0 mm, $t = t_0$ = 2.22 mm, and $R = t'$ = 0.75 mm; width in y-direction is 10 mm). The specimen was cut out using an electrical discharge machine.

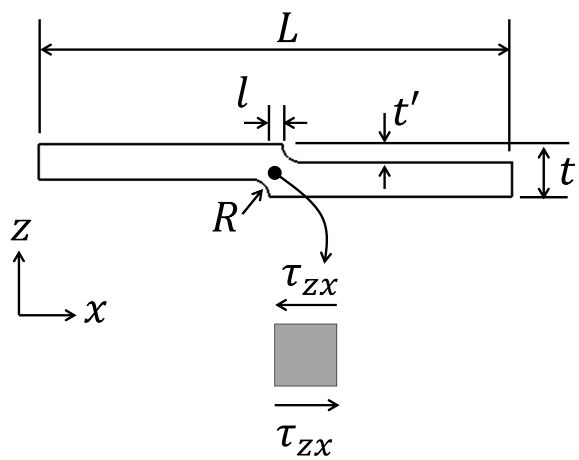

Figure 3 Geometry of the specimen.

Experimental condition. The testing apparatus used was the Autograph AG-50kN X plus (Shimadzu corporation). Fig. 3 shows the schematic of the experiment setup. A DIC system was used to measure the strain on the x–z plane of the specimen. Two cameras were used to capture the images. MultiDIC software [6] was used to calculate the strain distributions. The displacement d at ±10 mm from the center of the specimen in the longitudinal (x) direction was also calculated.

Materials Research Proceedings 41 (2024) 1144-1149 https://doi.org/10.21741/9781644903131-126

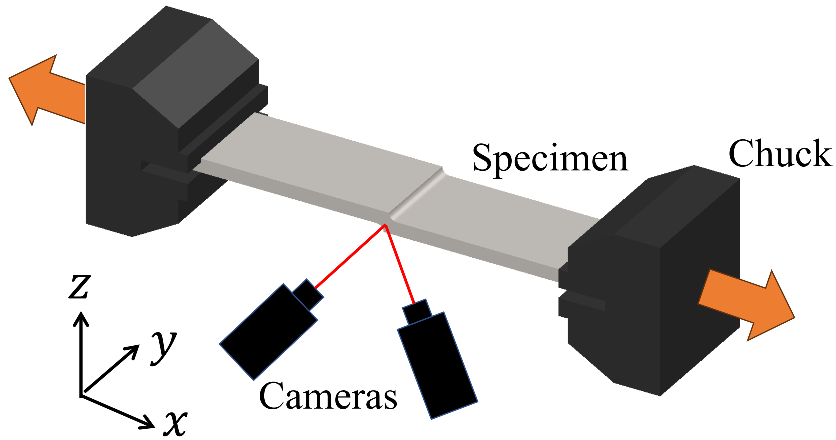

Figure 4 Schematic of the experimental setup.

Simulation conditions

3D-FEAs were performed to compare the deformation behavior with the experimental one. The shape of the specimen is affected by the precision of manufacturing process by electrical discharge machining. The contour shape of the specimen was measured using a microscope and reproduced by CAD. The software used in FEAs was Simufact Forming 2023 (Hexagon). A mesh window was set at the vicinity of the center of the specimen.

The simulation model is shown in Fig. 5. The material was assumed to be elastoplastic. The elastic properties were set as Young's modulus of 200 GPa and Poisson's ratio of 0.3. For the plastic properties, the work hardening law was eq. (1) and the Hill '48 yield function was used.

Only the parameter M of the Hill '48 yield function (Eq. (2)) was changed from 2.0 to 5.0 at the interval of 0.1 to find the the through-thickness shear anisotropy parameter to mimize the error between experiment and simulation. All other anisotropy coefficients were assumed to be isotropic ($F = G = H = 1$ and $L = N = 3$).

$$f = \frac{1}{2}\left\{F\left(\sigma_y - \sigma_z\right)^2 + G(\sigma_z - \sigma_x)^2 + H\left(\sigma_x - \sigma_y\right)^2 + 2L\sigma_{yz}^2 + 2M\sigma_{zx}^2 + 2N\sigma_{xy}^2\right\} \quad (2)$$

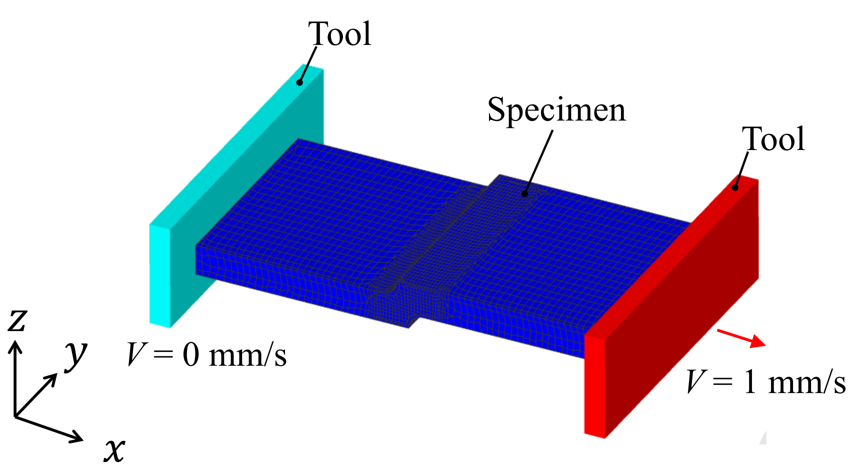

Figure 5 Simulation model.

Results and discussion

Shear strain–displacement curves. The variations of the through-thickness engineering shear strain γ_{xz} at the center of the specimen with increasing displacement *d* up to 0.5 mm are shown in Fig. 6. A shear strain of 0.02 can be attained in the experiment.

While the shear strain-displacement curve calculated using the parameter *M* = 3.5 agrees well with the one measured up to a displacement of 0.3, the calculated curve using *M* = 3.9 agrees well with the measured one over a displacement of 0.3. This behavior might be caused by the differential hardening [7].

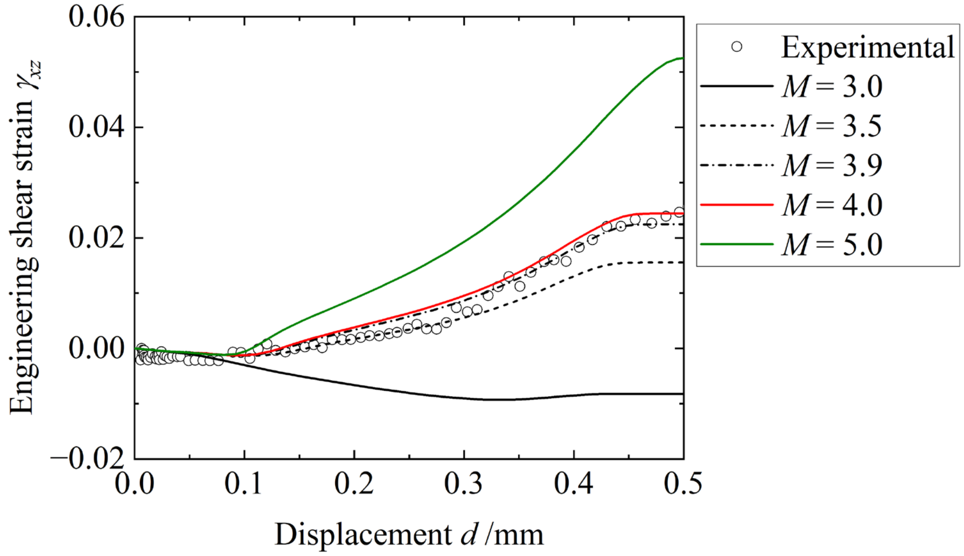

Figure 6 Measured and simulated shear strain-displacement curves.

Influence of shear anisotropy on the deformation behavior of plate forging. Plate compression analyses were performed using the simulation model shown in Fig. 1 and the conditions in the reference [2]. The yield function used is Hill '48 yield function. Two simulation was performed to evaluate the influence of shear anisotropy on the deformation behavior of plate compression. One is the through-thickness shear parameter *M* is set as the isotropic condition (*M* = 3.0). Another is *M* is set as the best parameter identified in the previous section (*M* = 3.9). The anisotropy parameters *F*, *G*, *H*, *L*, and *N* are set as the isotropic condition (*F* = *G* = *H* = 1 and *L* = *N* = 3).

Fig. 7 shows the distribution of the shear strain γ_{zx} at the compression ratio at the edge of 10 %. The maximum through-thickness shear strain for *M* = 3.9 is twice as large as that for *M* = 3.0. The anisotropy of through-thickness shear affects the deformation behavior of plate compression.

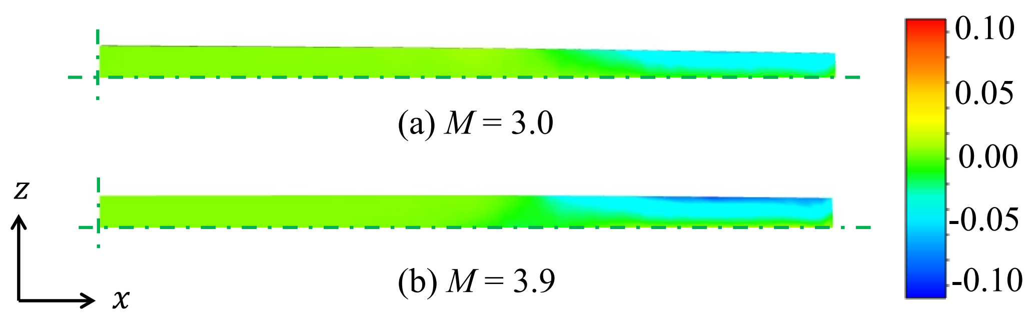

Figure 7 Distribution of engineering shear strain γ_{zx} at the compression ratio at the edge of 10 %.

Conclusions

(1) A through-thickness shear strain up to 0.02 can be attained by a tensile testing type material testing method.

(2) The parameters of the Hill '48 yield function were identified using the shear strain-displacement curves. The shear strain-displacement curve calculated using the parameter M = 3.5 agrees well with the one measured up to a displacement of 0.3. The calculated curve using M = 3.9 agrees well with the measured one over a displacement of 0.3.

(3) The anisotropy in the thickness direction affects the deformation behavior of plate compression.

Some material requires a high order yield function such as the Yld2004 yield function [8]. However since the number of the parameters increases to 2 for the Yld2004, it might be better to additionally evaluate the strain distribution in the specimen to identify the anisotropy parameters. The application of other materials is the future work.

Acknowledgment

This work was supported by the grants of THE AMADA FOUNDATION and the Ihara Science Nakano Memorial Foundation.

References

[1] M. Merklein, J.M. Allwood, B-A. Behrens, A. Brosius, H. Hagenah, K. Kuzman, K. Mori, A.E. Tekkaya, A. Weckenmann, Bulk forming of sheet metal. CIRP Ann. 61-2 (2012) 725–745. https://doi.org/10.1016/j.cirp.2012.05.007

[2] Z.G. Wang, T. Hakoyama, Y. Yoshikawa, Plastic deformation of workpiece during unloading in plate compression, CIRP Ann.-Manuf. Tech. 70 (2021) 223-226. https://doi.org/10.1016/j.cirp.2021.04.005

[3] T. Kuwabara, Advances in experiments on metal sheets and tubes in support of constitutive modeling and forming simulations, Int. J. Plast. 23-3 (2007) 385-419. https://doi.org/10.1016/j.ijplas.2006.06.003

[4] A. Lattanzi, M. Rossi, A. Baldi, D. Amodio, Development of new experiment test for sheet metals through-thickness behaviour characterization, Journal of Physics: Conf. Series 1063 (2018) 012040. https://doi.org/10.1088/1742-6596/1063/1/012040

[5] R. Hill, A theory of the yielding and plastic flow of anisotropic materials, Proceedings of the Royal Society A 193-1033 (1948) 281-297. https://doi.org/10.1098/rspa.1948.0045

[6] D. Solav, K. M. Moerman, A. M. Jaeger, K. Genovese and H. M. Herr, MultiDIC: An Open-Source Toolbox for Multi-View 3D Digital Image Correlation, IEEE Access 6 (2018) 30520-30535. https://doi.org/10.1109/ACCESS.2018.2843725

[7] R. Hill, J.W. Hutchinson,.Differential Hardening in Sheet Metal Under Biaxial Loading: A Theoretical Framework, ASME. J. Appl. Mech 59-2S (1992) S1–S9. https://doi.org/10.1115/1.2899489

[8] F. Barlat, J.C. Bream, J.W. Yoon, K. Chung, R.E. Dick, D.J. Lege, F. Pourboghrat, S.-H. Choi and E. Chu, Plane stress yield function for aluminum alloy sheets—part 1: theory, Int. J. Plasticity 19-9 (2003) 1297-1319. https://doi.org/10.1016/S0749-6419(02)00019-0